The 2013 World Congress on
Advances in Structural Engineering and Mechanics (ASEM13)
Jeju, Korea, September 8-12, 2013

The TiNi wires appropriate for damping of stayed cables in a standard and in extreme summer - winter temperature domain

F. Casciati[1], S. Casciati[2], V. Torra[3] and G.Carreras[3]

[1]*Structural Mech Dept., Universita degli study di Pavia, Pavia, Italy*
[2]*Dept. DICA, School of Architecture, University of Catania at Siracusa*
Piazza Federico di Svevia, I-96100 Siracusa, Italy
[3]*PRG, Villarroel 162, E-08036 Barcelona, Catalonia, Spain*

ABSTRACT

The experimental results obtained from NiTi SMA establish their appropriateness for damping the oscillations of stayed cables. The study establishes the necessary training, the fracture-life and the temperature effects and the self-heating actions. The stress-aging actions induce and useful increase of the maximal stress. The comparison between the results for different cables permits the formulation of the working rules for the application of the SMA in damping.
……

1. INTRODUCTION

The experimental results showed that the polycrystalline NiTi wires exhibited satisfactory characteristics for damping the oscillations of stayed cables (Torra et al. 2013a). In this paper, the analysis consists of four parts. The first focuses on mechanical actions: after obtaining appropriate lengths of 2.46 mm diameter wires, the wires must be initially trained. For instance, the training uses 100 working cycles at 0.01 Hz with a strain of 8 %. For such training, the SMA creep induced an irrecoverable increase of approximately 2 % in the length. Subsequent creep was practically negligible. After training, the coupling effects between the external cooling, the self-heating and the hysteretic shapes were reduced. The pauses realized between the series of working cycles induce minor creep recovery and produce local changes in the hysteretic behavior. Their action for larger numbers of working cycles was negligible. Using smaller deformations (i.e., below 1 or 1.5 %) resulted in an appropriate fracture-life that exceeded several million of working cycles. Part two relates the external temperature actions and the self-heating effects, in particular those induced by the strain and the cycling frequency. After training, the hysteretic shape was approximately S-shaped. This behavior can enable SMA dampers to be used “outside” in the Western Europe, i.e., between 253 and 313 K. Part three covers the effect of the stress-aging showing that a monotonic and permanent hysteretic shape changes up to 800-1000 MPa. The increase of available maximal stress favors the use of the SMA damper in climates as in South Canada or in Northern Europe (233 to 313 K). Part four focuses, by comparison between standard cables with thinner cable, on phenomenological rules for damper preparation to be adapted to each cable.

2. Part 1: mechanical action

The experimental analysis was focused in NiTi wires of 2.46 mm of diameter permitting stresses near 600 MPa and associate forces up to 3 kN. The figure 1A outlines the effect of training by 100 sinusoidal cycles at 0.01 Hz with a maximal strain of 8 %. The cycles induce a progressive SMA creep up to 2 % with an S-shape. Using a wire of 0.5 mm after 100 cycles (figure 1B) the hysteretic behavior remains flat. According to the Clausius-Clapeyron coefficient [near 6 MPa/K in (Isalgue et al., 2008)] the SMA remains in martensite for temperatures under 273K, without correct working for damping. The figure 1C shows the Basquin law (Basquin, 1910; Carreras et al. 2011; Casciati and Marzi, 2012) established by experimental measurements. The fit indicates that larger fracture life was associate to reduced stress, i.e., near 200 MPa. According to the possibilities of the used MTS the faster cycling requires reduced strains –as appropriated for fracture life- as, for instance, near 1%. The figure 2 was devoted to energetic (hysteretic) measurements at reduced strain (under 2.5 %). The figure 2A visualizes the hysteresis cycles for a progressive strain (from D to A). A parabolic fit, in figure 2B, was a satisfactory adjustment for strains under 2.5 % to the dissipated energy. In general, for a constant strain (1.5%) the energy decays by a linear fit against the cycling frequency. See, for instance, the figure 2C. At extremely reduced strains (under 0.5%), the frequency decay for partial loops seems not relevant.

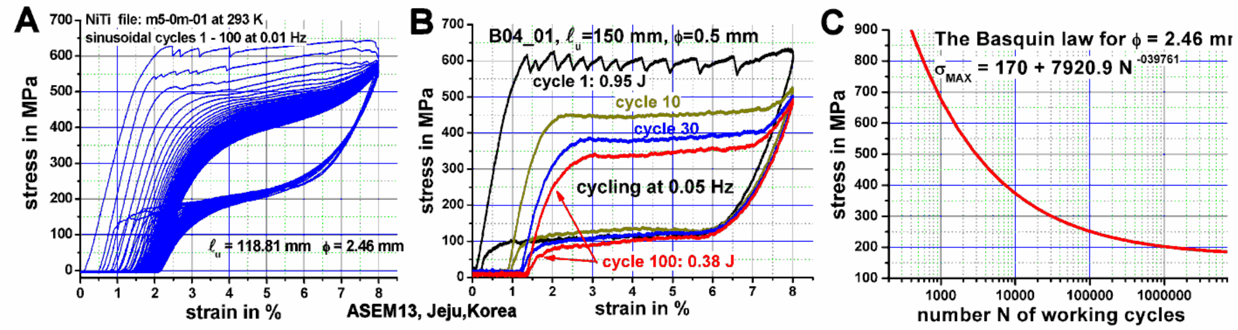

Figure 1. Cycling in NiTi wires. A: Wire of 2.46 mm. 100 sinusoidal cycles at 100 s with a strain of 8 % transforms the hysteretic behavior to S-shaped. B: Wire of 0.5 mm. Series of 100 cycles at 20 s. C: The fit of the Basquin law: Stress against the number of working cycles.

3. Part 2: temperature and self-heating actions.

The figure 3 relates the particular effects of self-heating. In figure 3A, cycling at 0.01 Hz and a maximal strain of 8% the sample temperature oscillates with the cycling action ± 8-10 K. In figure 3B, the frequency effect increases the mean temperature up to 25K at 3Hz. This temperature suggests that the stress increase more than 150 MPa with a relevant reduction of the working life. The figure 3C shows that minor strains (under 1 %) at higher cycling frequency (up to 16 Hz) only induce “minor” temperature increases.

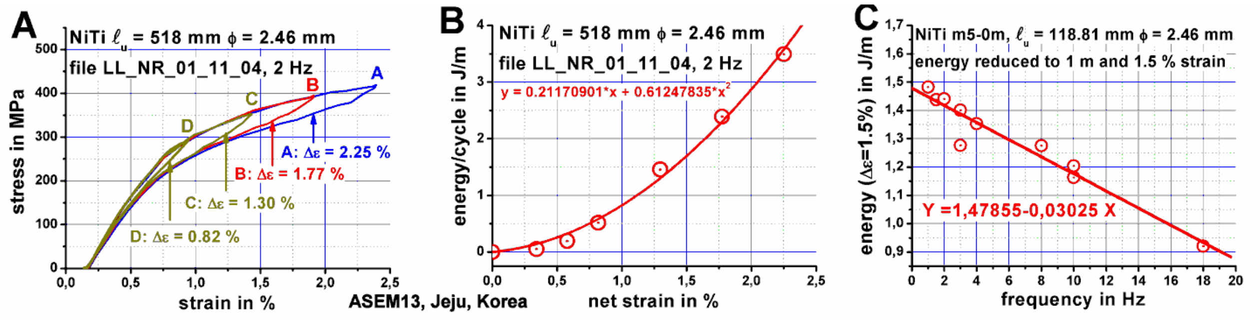

Figure 2. The hysteretic energy against deformation and frequency for 2.46 mm of diameter at reduced strains. A: Series of cycles realized at 2 Hz with deformation up to 2.25 %. B: Parabolic fit for the energies against the deformation. C: The measurements against the frequency for a strain of 1.5 % fit satisfactorily by one straight line.

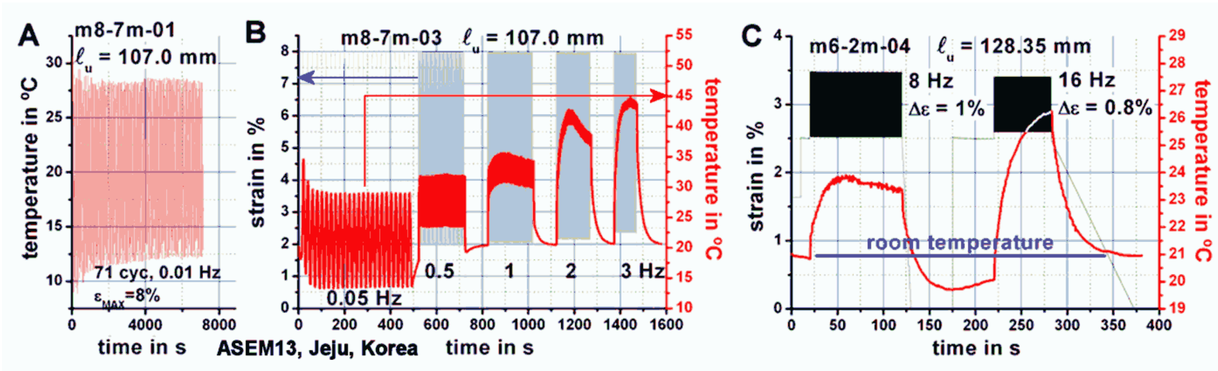

Figure 3. The sample temperature and the frequency effects. A: Changes in temperature for 8 % strain in cycles at 0.01 Hz. B: Strain (up 8 %) and temperature for progressive increased frequency (up to 3 Hz) for available strains between 2 and 8 %. C: Temperature effects for faster cycling and reduced deformation: cycling frequency at 8 and at 16 Hz for respective strains of 1 and 0.8 %.

The S-shaped cycle in NiTi of 2.46 mm permits reasonable behavior under the action of summer-winter temperature actions. The figure 4A shows the sample temperature (bottom) under continuous cycling at 0.05Hz with a maximal strain of 5% and the associated energy (top) for a previously cycled sample. In cooling to 258 K the sample remains, progressively, in martensite (cycles C and D in figure 4B). The experimental analysis suggest that the trained samples permits satisfactory work between 313 and 253 K.

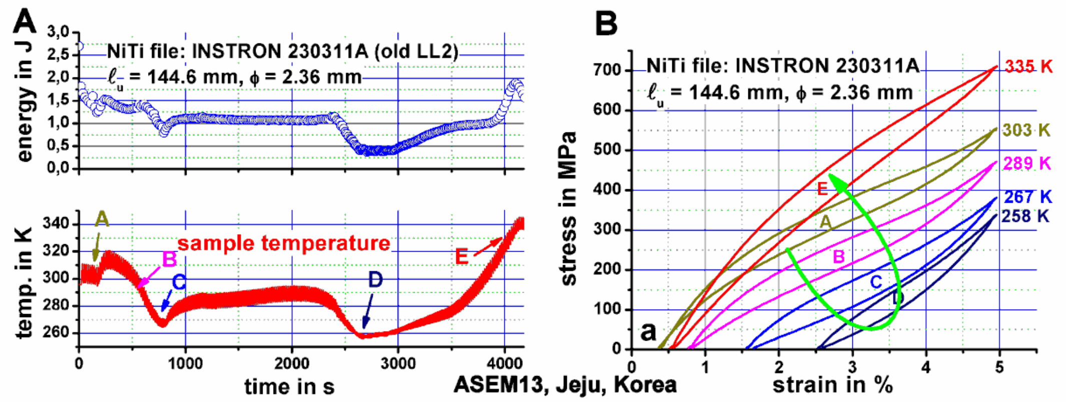

Figure 4. External temperature effects on cycling. A: Energy (top) and sample temperature (bottom) against time. B: Hysteresis cycles for several working temperatures. “a”: Grips adaptation. Arrow: hysteretic evolution associated to the effects of decreased and increased temperature, from cycle A to cycle E.

4. Part 3: The stress aging and the increase of the maximal stress.

Preliminary studies establish an evolution of the hysteretic behavior under aging at constant strain. An auxiliary equipment was prepared for aging samples at 373K under constant strain (figure 5 A and B). As the samples are cylindrical wires the device permits a mechanical analysis without dismounting and remounting, i.e., avoiding parasitic effects of the grips at the ends (figure 5B). Aging “as furnished” samples partially deformed (strain 4.5%) the first cycle was changed (figure 5C) but, after training the cycle 100 was, practically, the same those samples without stress aging. The aging effect was highly relevant for completely transformed samples with strain of 6.8%. The change remains after storing two years the samples at room temperature. Cycling reduces the hysteresis shape but the maximal stress increases to 900 MPa. According the results visualized in figure 4 the strain-aged samples permits satisfactory work for temperatures as low as 238K.

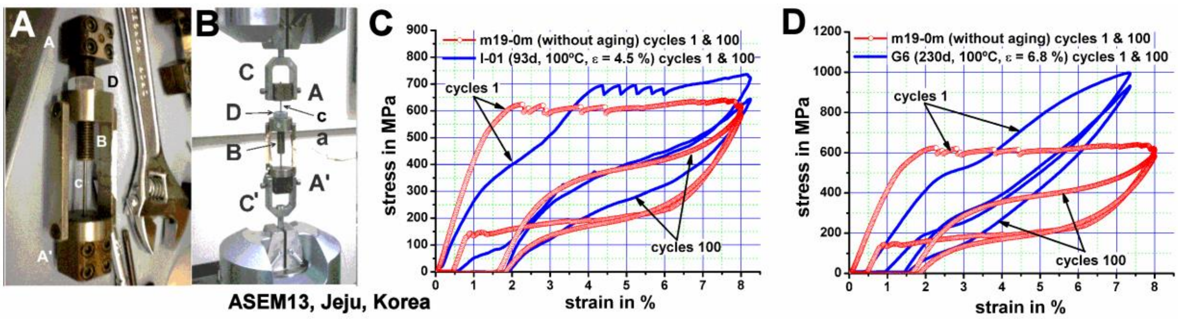

Figure 5: A: adapted device for stress-temperature aging. A and A’: the cubes that fasten the ends of the sample “c”. B and D: screw and the associate bolt that allows to modifying the length of the sample by stress. B: positioning of the device when working in traction using conventional equipment (i.e., a MTS 810). C and C’: auxiliary grips. “a”: room temperature thermocouple. C and D: Effects of the stress aging at 373 K in “as furnished” samples. C: The strain value was 4.5 % and 93 days of aging. D: The strain value was 6.8 % and 230 days of aging.

5. Part 4: The experimental measurements permitting an approach to dampers

An experimental study of the SMA wires efficiency in damping was realized in ELSA using the 45 m cable Number 1 (four steel sets of wires and wax inside a polyethylene tube). The figure 6A shows the effect of the one trained SMA wire (s079 with a length near 4000 mm) in a free oscillation (s071) (Torra et al., 2013b). The local evolution of frequency induced by the changes in the SMA force related to the oscillations amplitude (dots). The figure 6B shows the mean frequencies without and with the SMA determined by the FFT. The figure 6C outlines a complete simulation: cable without wax, with wax and with SMA.

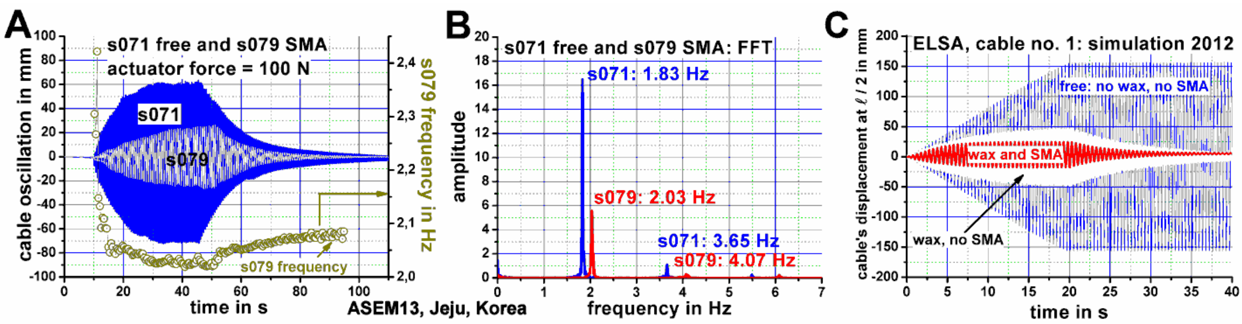

Figure 6. ELSA, cable No 1: experimental ELSA cable oscillations (measurements s071 and s079). A: equal excitation (98 N) at resonance frequencies without (s071) and with (s079) SMA damper. Dots: direct calculation of the frequency against time in the measurement s079. B: frequencies determined by the FFT with a 10 % of change. C: Outline of the simulation without wax was (unavailable from experiments), with wax (free cable) and with a damper by only one wire of SMA.

In the Pavia Laboratory using a 2 mm steel wire loaded with lead balls the effect of a SMA wire of 0.1 mm was relevant (figure 7A). The experimental observations include higher noisy signals. The FFT frequency determined from the signal decays changes a 20-25%. The figure 7C shows an outline of the simulation and of the SMA effect.

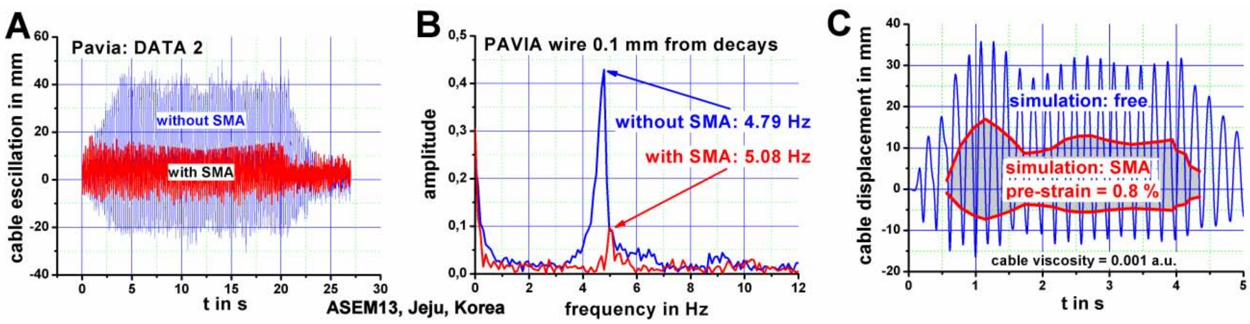

Figure 7. Experimental and calculated results in the Pavia cable. A: effect of the SMA damper on the oscillations amplitude. B: frequency spectrum determined from the decays in A. C: Outline of the calculated oscillations and of the SMA effect.

Table 1 shows the available data for the cable No 1 in ELSA and for the indoor cable at the Pavia University, which was used to provide an extreme comparison.

Table 1. Comparison between dampers in ELSA and Pavia.

facility.	L m	SMA (wires)	length( ) mm	NiTi SMA in mm	(cable) in MPa	traction force	f_{SMA} near	cable diameter	x mm	f Hz
ELSA	45	1	4140(*)	2.46	283	250 kN	1.5 kN	4*15 mm	60	2
Pavia	2.36	1	1229(**)	0.1	43	133.8 N	2 N	2 mm	40	5

(*) appropriate length with larger fracture life.
(**) thinner wire: the fracture life requires deeper study

A SMA damper should be constructed to realize the desired damping action in a well known cable permitting, eventually, a reliable simulation. Two requirements are mandatory for an appropriate and efficient damper. The first one was the SMA length, associate to a large number of working cycles. Let “x” denote the acceptable residual amplitude after damping. The required length ( ) for the SMA wires, which ensure that the oscillation amplitudes do not exceed 1 %. The length ( ) can be related to the oscillation amplitude (x) as follows

$$0.010 \qquad = x(NiTi) \tag{1}$$

The second one compares the SMA force and the dynamic forces in the cables in an extremely rough estimate. These forces were considered to act in the same direction in the SMA position. The basic idea considers that the ratio of the dynamic forces in the cables, which are associated with the oscillation amplitude, the frequency and the cable mass, were similar to the force ratio in the SMA dampers. The ratio between the cross-sections could be considered using the ratio between the SMA wires (N) multiplied by the cross-section. The ratios between the Pavia cable and the ELSA cable were as follows:

$$Dynamic\ \ force\ ratio = \frac{F_{Paviacable}}{F_{ELSAcable}} = \frac{(\rho\ \pi\ r^2 L\ \omega^2\ \Delta x)_{Paviacable}}{(\rho\ \pi\ r^2 L\ \omega^2\ \Delta x)_{ELSAcable}} = 0.0012$$

$$\frac{force_{SMA\,Paviacable}}{force_{SMA\,ELSAcable}} = \frac{\left(\pi * r^2\right)_{SMA\,Paviacable}}{\left(\pi * r^2\right)_{SMA\,ELSAcable}} = 0.0016 \tag{2}$$

The calculated ratios show that the proposed approach is fairly satisfactory. To identify the two ratios, the SMA cross-section for a new damper is calculated as follows:

$$\frac{F_{newcable}}{F_{ELSAcable}} = \frac{force_{SMAnewcable}}{force_{SMAELSAcable}} = \frac{cross\ section_{SMAnewcable}}{cross\ section_{SMAELSAcable}} \Rightarrow$$

$$cross\ section_{SMAnewcable} = \left(\pi * r^2\right)_{SMAELSAcable} \frac{(\rho\ \pi\ r^2 L\ \omega^2\ \Delta x)_{newcable}}{(\rho\ \pi\ r^2 L\ \omega^2\ \Delta x)_{ELSAcable}} \tag{3}$$

Using wires with the same diameter (2.46 mm) the number N of SMA wires in the new cable is given by

$$\frac{force_{SMAnewcable}}{force_{SMAELSAcable}} = \frac{N\ \left(\pi * r^2\right)_{SMAnewcable}}{\left(\pi * r^2\right)_{SMAELSAcable}} = N \tag{4}$$

Using formula (5), the number (N) of SMA wires with equal diameters is given by

$$N = \frac{F_{newcable}}{F_{ELSAcable}} = \frac{(\rho\ \pi\ r^2 L\ \omega^2\ \Delta x)_{newcable}}{(\rho\ \pi\ r^2 L\ \omega^2\ \Delta x)_{ELSAcable}} \tag{5}$$

4. CONCLUSIONS

The experimental results showed that the polycrystalline NiTi wires exhibit satisfactory characteristics for damping the oscillations of stayed cables. After obtaining appropriate lengths of 2.46 mm diameter wires, the wires must be initially trained using 100 working cycles with a strain of 8 % and 0.01 Hz. For such training, the SMA creep induces an irrecoverable increase of approximately 2 % in the length. Subsequent creep was practically negligible. After training, the coupling effects between the external cooling, self-heating and the hysteretic shapes were reduced. Using smaller deformations (i.e., below 1 or 1.5 %) the fracture-life was appropriate: remains close to several million of working cycles.

The hysteretic shape after training was approximately S-shaped. This behavior can enable SMA dampers to be used outside in the Western Europe, i.e., for climates with temperatures between 258 and 313 K. Stress-aging studies have shown that a monotonic and permanent hysteretic shape change up to 800-1000 MPa can enable a SMA damper to function in more stronger climates as in South Canada and in North Europe (233 to 313 K). Simulation of the cable behavior required the use of the cubic model and appropriate rules to build internal loops. The classical bilinear model cannot be used for small deformations, i.e., for strains below 1 %. Comparing the behavior of the standard ELSA with the thinner cable at Pavia University enabled rules for damper preparation to be formulated that can be adapted to any cable.

REFERENCES

Basquin, O.H., (1910), “The exponential Law of endurance tests”. Proc Am Soc Test Mater Proc , 625-630.

Carreras, G., Casciati, F., Casciati, S., Isalgue, A., Marzi, A., Torra V. (2011), “Fatigue laboratory tests toward the design of SMA portico-braces”. *Smart Structures and Systems*, 7(1) 41- 57.

Casciati, S., Marzi A. (2012), “Experimental studies on the fatigue life of shape memory alloy bars”, *Smart Struct Syst* 6 (1) 73-85.

Isalgue A, Torra V, Yawny A, Lovey FC. (2008), “Metastable effects on martensitic transformation in SMA Part VI. The Clausius–Clapeyron relationship.” *J Thermal Anal Calorim* 91(3) , 991–998.

Torra, V., Isalgue,A., Auguet, C., Carreras, G., Lovey, F.C., Terriault P. (2013a), “Damping in Civil Engineering using SMA. Part II. Particular properties of NiTi for damping of stayed cables in bridges”, *Canadian Metallurgical Quarterly*, 52 (1), 81-89

Torra, V., Auguet, C., Isalgue, A., Carreras, G., Terriault, P., Lovey F.C.(2013b), “Built in dampers for stayed cables in bridges via SMA. The SMARTeR-ESF project: A mesoscopic and macroscopic experimental analysis with numerical simulations”, *Engineering Structures* 49 43–57.